Geophysica (2018), 53(1), 45–64

Automated Measurements of Snow on the Ground in Sodankylä

Leena Leppänen, Anna Kontu and Jouni Pulliainen

Finnish Meteorological Institute
Space and Earth Observation Centre, Sodankylä, Finland

(Submitted: June 25, 2018; Accepted: November 26, 2018)

Abstract

Automated in-situ snow measurements allow for continuous observations and extensive measurement networks into unpopulated areas. The collected information of essential snow parameters (e.g. snow water equivalent (SWE) and snow depth) is important for weather prediction, climate modelling and interpretation of remote sensing observations. The Arctic Space Centre of Finnish Meteorological Institute in Sodankylä has several field experiment sites, where automated and manual snow observations are performed e.g. for the purposes of operational weather services and development of remote sensing applications. The first automated snow measurements in Sodankylä were snow depth and snow temperature profile installed in 2000. The major snow observations were established in 2006, when tower-based optical radiance measurements and manual snow pit measurements started. Automated reference measurements including snow on the ground observations were installed following this. Tower-based microwave observations have been made since 2009 for remote sensing related purposes. The three measurement sites, the Intensive Observation Area, the bog site and the Integrated Carbon Observation System (ICOS) tower site, have hosted the tower-based observations, and most of the automated in-situ snow measurements. In addition, the WMO Solid Precipitation Intercomparison Experiment (SPICE) had a measurement site in Sodankylä in 2013–2015, involving several automatic snow on the ground instruments measuring snow depth and SWE. In this study, the automated snow depth, SWE and snow temperature profile measurements are compared with the manual observations to study the accuracy of the automated measurements. For the examined periods, the correlation of observations is strong with correlation coefficients between 0.93 and 0.96, p-values of <0.001, and average bias around 10 % for the snow depth (absolute bias of 7.9 cm) and snow temperature (absolute bias of 0.3 °C) and approximately 2 % for SWE (absolute bias of 1.0 mm).

Keywords: field observations, boreal forest, snow, remote sensing

1 Introduction

Snow cover is vital as a source of fresh water for a fifth of the Earth's population (*Barnett et al*., 2005). Seasonal snowpack is a reservoir of wintertime precipitation and releases all the water in a short period of time, which may cause flooding (e.g. *Bell et al*., 2016, *Vormoor et al*., 2015). The accumulation of snow on mountains may lead to avalanches (e.g. *Lehning et al*., 1999). Due to numerous strong feedback mechanisms between snow and climate, snow cover is an important but yet poorly known factor in climate change (*Xie et al*., 2015; *Hall and Qu,* 2006). The most essential measured snow parameters are the snow depth and the snow water equivalent (SWE). SWE describes either the weight of snow on one m^2 (unit kg m^{-2}) or depth of water obtained, if the whole snowpack is instantaneously melted (unit mm), so that the numerical values are the same for both of the units. Automated in-situ snow measurements allow continuous

observations at unmanned stations. A wide network of automated observations provides important information for the forecasting of weather, floods and avalanches (*de Rosnay et al*., 2012) as well as for the purposes of climate change research (e.g. *Hernández-Henríquez et al*., 2015) and the interpretation of satellite observations (*Takala et al*., 2017). The precision of remote sensing observations depends on the interpretation method (e.g. *Rittger et al*. 2013). The ground-based optical and microwave observations are essential for the development of remote sensing retrieval algorithms (e.g. *Lemmetyinen et al*., 2016b; *Maslanka et al*., 2016; *Salminen et al*., 2009).

The reference snow in-situ measurements and tower-based microwave and optical observations at the Arctic Space Centre of the Finnish Meteorological Institute (FMI-ARC, previously called Arctic Research Centre) focus on providing information for validation, calibration and development of satellite based remote sensing instruments and interpretation algorithms (e.g. *Pulliainen et al*., 2014, *Lemmetyinen et al*., 2015, *Maslanka et al*., 2016, *Rautiainen et al*., 2016). This paper describes the automated measurements of snow on the ground. In addition, automated measurements of snowfall are performed at FMI-ARC. The manual snow measurements, including snow pit, snow course, snow depth and SWE measurements, are described in *Leppänen et al*., (2016), which also describes in detail the measurement sites of FMI-ARC with listing of all automatic instrumentation at the sites. The observations of snow cover are complemented with soil temperature and soil moisture measurements (*Ikonen et al*., 2015, *Rautiainen et al*., 2014), which are needed to describe the background in snow microwave emission modeling and also provide information on soil frost status and depth.

Some comparisons of the automated SWE and precipitation measurements at the FMI-ARC in Sodankylä have been published. The World Meteorological Organization (WMO) arranged a Solid Precipitation Intercomparison Experiment (SPICE) in 2012–2015 for the purpose of evaluating automated instruments available for solid precipitation measurements in different environments and climate conditions. One component of the experiment was snow on the ground, which compared instruments for snow depth and SWE measurements to manual reference measurements. The site at FMI-ARC hosted several automated instruments to measure precipitation, snow depth and SWE. The results will be presented in the SPICE Final Report. *Smith et al*. (2017) compared automated SWE measurements with manual reference observations made at the Sodankylä SPICE site in 2013–15. The CS725 (Campbell Scientific) overestimated SWE on average by 30% and the SSG1000 (Sommer Messtechnik) underestimated SWE on average by 11% compared to the manual reference observations. Automatic Pluvio2 (OTT Hydromet) and VRG101 (Vaisala) accumulating precipitation gauges were compared with manual H&H-90 precipitation measurements at Sodankylä in *Janowicz et al*. (2017). In addition, previous studies have compared microwave observations of FMI-ARC presented in *Lemmetyinen et al*. (2016b) with simulations based on in-situ snow observations (*Maslanka et al*., 2016; *Kontu et al*., 2017; *Sandells et al*., 2017; *Lemmetyinen et al*., 2018). Tower-based optical reflectance observations have been compared with in-situ reflectance observations in *Salminen et al*. (2009).

The data from automated snow measurements at FMI-ARC is available at http://litdb.fmi.fi. The data collected for SPICE (including also snow depth and SWE observations) is not yet available, but will be made available after publication of the SPICE Final Report. The data sets of microwave instruments and GWIs are available on request (contact information is available at http://litdb.fmi.fi). The availability of manually measured data is described in *Leppänen et al*. (2016). The header rows of the data files downloaded from the website include station name, date, UTC time, parameters and units. Other metadata (sensor types, parameters, data availability periods and station coordinates) is described on the website.

The aim of this paper is to present the automated measurements of snow on the ground at FMI-ARC in Sodankylä, Finland, and to compare the automated observations with the manual measurements to study the precision of the automated observations. In the paper, first the measurement sites and automated instrumentation are presented, then the automated and manual observations are compared, and the results are discussed.

2 Methods

2.1 Measurement sites

The FMI-ARC is located in northern Finland (67.367 N, 26.629 E). Typically, ground is covered with snow from October to May, and the maximum snow depth (on average 79 cm) occurs in March based on the 1981–2010 meteorological statistics (*Pirinen et al*., 2010). Wind speed is typically low, 2.2 m s^{-1} above tree tops and 1.2 m s^{-1} at 1.5 m height (*Leppänen et al*., 2016).

The six measurement sites at the FMI-ARC area (Intensive Observation Area (IOA), bog site, Integrated Carbon Observation System (ICOS) tower site, sounding station, meteorological mast, and SPICE site) for the automated snow measurements are marked in Fig. 1. Operational daily snow measurements have been made since 1908 in Sodankylä (*Tietäväinen et al*., 2010) and since 1913 in the FMI-ARC area, first manually and since 2008 using automated instruments. The location of the operational meteorological observations is the sounding station, which was built in 1949. Tower-based microwave measurements and manual snow pit measurements have been performed at the IOA, the bog site and the ICOS tower site. The IOA is covered with sparse pine forest, but most of the instruments were on a forest clearing. The bog site is an open peat bog with low vegetation. The ICOS tower site is in a pine forest close to the IOA. The total height of the tower is 24 m allowing installation of instruments well above tree tops. Main measurements in and around the tower are the carbon flux measurements following the ICOS standards. The meteorological mast site is close to the ICOS tower and the IOA, and is covered with similar sparse pine forest as the other sites. The SPICE site hosted several instruments in 2012–2015 during the intercomparison experiment. The instruments were installed on a forest clearing around a satellite receiving antenna. In addition, the Saariselkä area, ~200km north from Sodankylä, hosts several measurement stations with automated snow depth and broadband albedo measurements. Saariselkä area is open tundra with some small trees and differs from the FMI-ARC sites. The sites

at FMI-ARC in Sodankylä are described in detail (e.g. soil type, vegetation, automatic instrumentation) in *Leppänen et al*., (2016), with the exception of the recently established ICOS tower site. The automated snow measurements at each site are listed in Table 1 and described in the next chapters.

Table 1. Automated instruments for snow on the ground observations at the FMI-ARC sites. If more than one sensor is installed in the same year at a site, the number of instruments installed is in the parenthesis after the year.

Variable	Instrument	Method	IOA	Bog	ICOS tower	Sounding station	SPICE	Meteorological mast	Saariselkä
Snow depth	SR50	Ultrasonic	2006- (2)	2010-		2008-	2012-	2000-	2011-, 2014-
	SHM30	Laser ranger					2013-		
	USH-8	Ultrasonic					2012-2015 (2)		
	SL300	Ultrasonic					2012-2016		
SWE	GWI	Gamma radiation	2007-2014	2009-2016					
	SSG1000	Weighing scale	2015-2018		2018-		2013-2015		
	CS725	Gamma radiation					2013-2015		
Snow temperature	Thermometer profile		2011-	2012-				2000-	
Albedo	Albedometer CMA11	285-2800 nm	2010-	2011-					
	AlbedometerCNR4	300-2800, 4500-42000 nm							2012- (2)
Brightness temperature	ESA ELBARA-II	1.4 GHz	2009-2012, 2015-	2012-2015	2018- (2)				
	SodRad1	10.6, 18.7, (21), 36.5, (89) GHz	2009-2018		2018-				
	SodRad2	89, 150 GHz	2012-2016						
Back- scattering	ESA SnowScat	9-18 GHz	2010-2013						
	SodScat	1-10 GHz	2017-		2018-				
Radiance	Field Spec Pro JR	350-1000 (2500) nm	2006-						

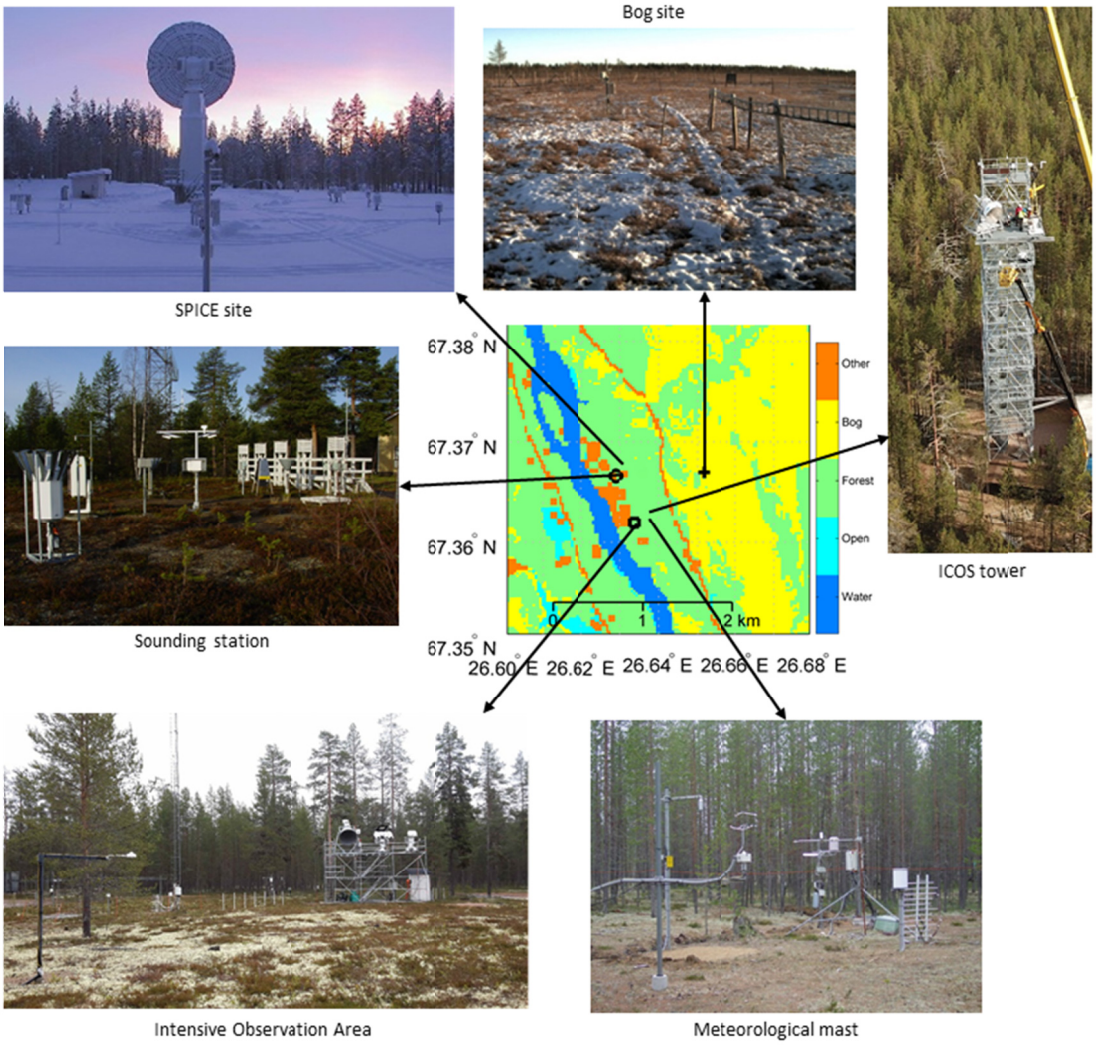

Fig. 1. Map of FMI-ARC area. Locations of the measurement sites are indicated with the arrows.

2.2 Snow depth measurements

Continuous automated snow depth measurements are made with acoustic ultrasonic SR50 sensors (Campbell Scientific) installed at 2-m height at automated weather stations (Fig. 2a). The same sensor is used in all FMI operational weather stations. The measurements have been made since 2000 in several locations listed in Table 1. The measurement is made every minute and 10 min average value is recorded. The measured target is artificial turf. Methods for data quality control are station dependent (e.g. varying water level at bog site needs special procedures), but the most common methods are visual check to detect outliers and automated removal of values with standard deviation over 10 cm in 10 min.

Several automated snow depth sensors were tested at the SPICE site in 2012–2015. The ultrasonic sensors deployed were the SR50ATH (Campbell Scientific), USH-8 (Sommer Messtechnik) and SL300 (Felix). An SHM30 (Luft/Jenoptik) laser ranger sensor was also installed. The laser-based SHM30 makes a point measurement, while the ultrasonic sensors have a larger field of view. The ultrasonic sensors detect the highest point (the first echo) in the field of view as the snow depth, while the laser measures

snow depth in one point. The representativeness and accuracy of both methods depend on snow surface structure and quality. If snow accumulates on sensors, it may drop to the field of view and either increase (a pile on surface) or decrease (a hole in snow) measured snow depth. In addition, densely packed snow may melt slower than freely accumulated snow. Snow accumulation on sensors can be avoided by heating the support poles, by installing the poles in 45° angle allowing snow to slide of the pole and by minimizing sensor surface area. Different sensor mountings were tested during SPICE to reduce snow accumulation on mounting structures.

2.3 SWE measurements

Automated SWE was measured continuously with the Gamma Water Instrument (GWI) (Astrock) at the IOA and the bog site (Fig. 2b). The GWI is an experimental prototype senor (not commercially available), which measures gamma radiation from a Cesium source installed at the ground level below the sensor. The SWE observation is based on the attenuation of gamma radiation by water in snow. The measurement takes approximately 10 min and it is made every 20 min. The instrument needs calibration with occasional manual SWE measurements. In addition, raw data needs processing prior to SWE derivation. The quality check is made visually. The first GWI was installed at the IOA in 2007–2014 and the second at the bog site in 2009–2016.

The CS725 (Campbell Scientific) was tested at the SPICE site in 2013–2015. The CS725 measurement is similar to the GWI and based on the attenuation of gamma radiation in snow, but it uses the natural radioactive elements in the soil as the source of the radiation (*Smith et al*., 2017). The CS725 observation requires soil moisture calibration prior to snow accumulation, and changes in soil moisture and liquid water in and below snowpack may induce inaccuracy in the measurements, especially during the melting period (*Smith et al*. 2017). Maximum measurable SWE is reported to be 600 mm by the manufacturer, which is not reached in Sodankylä. The recorded data was an average from continuous measurements with 24 h integration time.

SSG1000 (Sommer Messtechnik) was installed at the SPICE site in 2013–2015 and was then moved to the IOA (Fig. 2c) and to the ICOS tower site in 2018. The SSG1000 is based on load cells which measure the weight of snow over an underlying platform (*Smith et al*., 2017). The measurement is made every minute and quality control is made visually to detect incompatible values. Weighing snow sensors are sensitive to ice bridging (e.g. *Engeset et al*., 2000), when hard melt-freeze crust layers support the weight of snow and cause underestimation of SWE. Ice bridging can be detected by comparing automated measurements to manual measurements. The installation of the SSG1000 instrument should be on the ground level to reduce uneven accumulation compared to surroundings. GWI and CS725 have no similar problems due installation above the snow surface.

2.4 Temperature profile measurements

Temperature profile of the snowpack is measured continuously with thermistor probes (Campbell 107-L or Pentronic PT100). The measurements have been made since 2000 at the meteorological mast, since 2011 at the IOA and since 2012 at the bog. The sensors are installed every 10 cm between 0 cm and 110/120 cm. The accumulation of snow on the sensor rods and the formation of pits under the sensors was a problem at the IOA, and in 2015 the sensors were installed in three different poles at 30 cm intervals (Fig. 2d). The windy conditions at the bog site alleviate snow accumulation problems (Fig. 2e). The temperature sensors record data every 10 min, even when they are not covered with snow (i.e. exposed to the atmosphere). The snow depth data from closest SR50 sensor can be used to determine which temperatures are from inside and which from above the snowpack. Methods for data quality control are station dependent, but visual check and automated remove of values over 50 °C are the most common ones.

Fig. 2. a) A weather station with an SR50 sensor in sparse pine forest at the IOA, b) GWI at in forest clearing IOA and c) SSG1000 at IOA. Snow temperature profiles d) at IOA (installation every 30 cm in three poles) and e) at bog site (installation every 10 cm).

2.5 Radiation measurements

2.5.1 Broadband albedo measurements

Broadband albedo, which is highly dependent on the fractional snow coverage, is measured with two types of sensors: CMA11 and CNR4 (Kipp & Zonen). One CMA11 albedometer is installed at the IOA and one at the bog (Fig. 3a). The two CNR4 radiometers are installed at Saariselkä stations. The CMA11 measures the albedo with two pyranometers combined into one instrument with wavelength range 285–2800 nm. The CNR4 net radiometer measures the energy balance between incoming short-wave (300–2800 nm) and long-wave far infrared (4500–42000 nm) radiation versus surface-reflected short-wave and outgoing long-wave radiation. The CNR4 net radiometer consists of a pyranometer pair measuring the short-wave radiation, one facing upward, the other facing downward, and a pyrgeometer pair in a similar configuration measuring long-wave radiation. The measurement is continuous and the data is recorded every 10 min. Methods for data quality control are station dependent, but the most common procedures are visual check and automatic removal of outgoing radiation values that are larger than the incoming radiation values.

2.5.2 Spectral radiance measurements

Spectral reflectance at visual and near infrared wavelengths is dependent on the fractional snow cover, which is important for mapping of it, especially during the melting season. The Field Spec Pro JR (Analytical Spectral Devices) is a spectroradiometer with a fiber optic cable for signal collection. The instrument was installed in 2006 on a 30-m mast at the IOA (Fig. 3b) (*Niemi et al*., 2012, *Salminen et al*., 2009, *Sukuvaara et al*., 2007), and the system was fully automatized in 2012. The radiance was measured with 350–2500 nm wavelengths until 2015, after that only wavelengths 350–1000 nm are used. The fiber optic cable is on a rotating pole allowing measurements of different areas around the tower (forest and clearing). From 2013 onwards, only the forest area is measured. The head of the fiber optic cable is tilted 11° off nadir (away from the mast) to reduce noise from the mast. The data is recorded with various intervals depending on prevailing weather conditions and measurement procedures. Strong wind, rain or low illumination conditions prevent measurements. The visual quality control is made for the observed data.

2.5.3 Microwave brightness temperature measurements

Microwave emission is measured with three microwave radiometers: ESA ELBARA-II, SodRad1 and SodRad2, each having different frequency channels (Fig. 3c). The radiometric measurements are made with various intervals depending on prevailing measurement procedure. Typical measurements include 2D scans of snow at incidence angles between 30° and 70°. Data quality is controlled by continuous internal calibration with noise diodes. The SodRad radiometers require absolute calibration using targets at ambient temperature and in liquid nitrogen, and checks using only ambient

temperature targets. Too high and low values and outliers are removed from the data using visual inspection. The ESA ELBARA-II radiometer has an internal Active Cold Load (ACL) target, which is calibrated against sky measurements. In addition, semi-automated scripts check the data for too high and too low values, interference, differences between H and V polarization in sky measurements, temperature instability and outliers. The lower frequencies penetrate deeper in the snowpack than the higher frequencies. SWE can be retrieved from the observations of frequencies below 90 GHz with snow microwave emission models (e.g. *Wiesmann and Mätzler*, 1999; *Lemmetyinen et al*., 2010). The two highest frequencies observe radiation originating from the surface of the snowpack. The observations could be comparable with optical instruments, and related experiment will be conducted in 2019.

The ESA ELBARA-II is an L-band radiometer owned by the European Space Agency (ESA) and built by Gamma Remote Sensing (*Schwank et al*., 2010, *Rautiainen et al*., 2012). It measures both horizontal (H) and vertical (V) polarizations of 1.4 GHz microwave radiation. The radiometer has automated elevation positioner. The installation at ICOS tower allows for azimuth turning. The ESA ELBARA-II was at IOA in 2009–2012 and 2015–2018, and at bog site in 2012–2015 on 4–5 m high towers. In 2018, the ESA ELBARA-II was installed in the ICOS tower at 21-m height platform. Another similar upwards-looking ESA ELBARA-II instrument with a manual azimuth turning system was simultaneously installed on the ground level. The L-band radiometer detects soil moisture and soil frost, but dry snow is also visible in the observations (*Lemmetyinen at al*., 2016a).

SodRad1 and SodRad2 are commercial radiometers (RPG-8CH-DP and RPG-4CH-DP) built by Radiometer Physics GmbH (*Lemmetyinen et al*., 2016b). The SodRad1 measured in 2009–2018 and the SodRad2 in 2013–2016 on a 4 m high tower at the IOA. The SodRad1 was installed to the ICOS tower at 21-m platform in 2018 and SodRad2 will be installed to the bog site in the beginning of 2019. The SodRad radiometers measures horizontal and vertical polarizations and are able to scan in both azimuth and elevation directions. The SodRad1 originally had frequencies 10.6, 18.7, 36.5 and 89 GHz. In 2011, the 89 GHz receiver was replaced with a 21 GHz receiver, and the 90 GHz receiver was integrated with a 150 GHz receiver into SodRad2.

2.5.4 Microwave backscattering measurements

Microwave backscattering can be related to snow properties, e.g. SWE can be determined by a backscattering model (*Lemmetyinen et al*., 2016b) or by differential interferometry (*Leinss et al*., 2015). Microwave backscattering was measured with the ESA SnowScat scatterometer in 2009–2013 and the SodScat scatterometer in 2017 at the IOA, and SodScat was installed to the ICOS tower in 2018. The scatterometers were mounted on an 8-m high tower at the IOA. ESA SnowScat is an X- to Ku-band scatterometer owned by ESA and built by Gamma Remote Sensing AG (Fig. 3d) (*Wiesmann et al*., 2010, *Lemmetyinen et al*., 2016b). It was attached to a support beam about 1 m outside the tower structure so that it was able to perform both elevation and azimuth scans. For system performance control, an external calibration target was used, which

was a metal sphere with a radius of 10.16 cm mounted on a bar at the target area. The SodScat scatterometer is built by Harp Technologies around a vector network analyzer (VNA) manufactured by Agilent Technologies (Fig. 3e). The scatterometer uses frequencies 1–10 GHz with both horizontal and vertical polarizations. The scatterometer was installed at a constant angle without the possibility for elevation or azimuth scanning at the IOA. The installation onto the ICOS tower below 21-m high platform in 2018 included a rail and turning system to allow elevation and azimuth scans and horizontal movement of the scatterometer. The external calibration target is a sphere with 20 cm diameter. The measurements are made with various intervals depending on prevailing measurement procedure. Method for the data quality control is visual check.

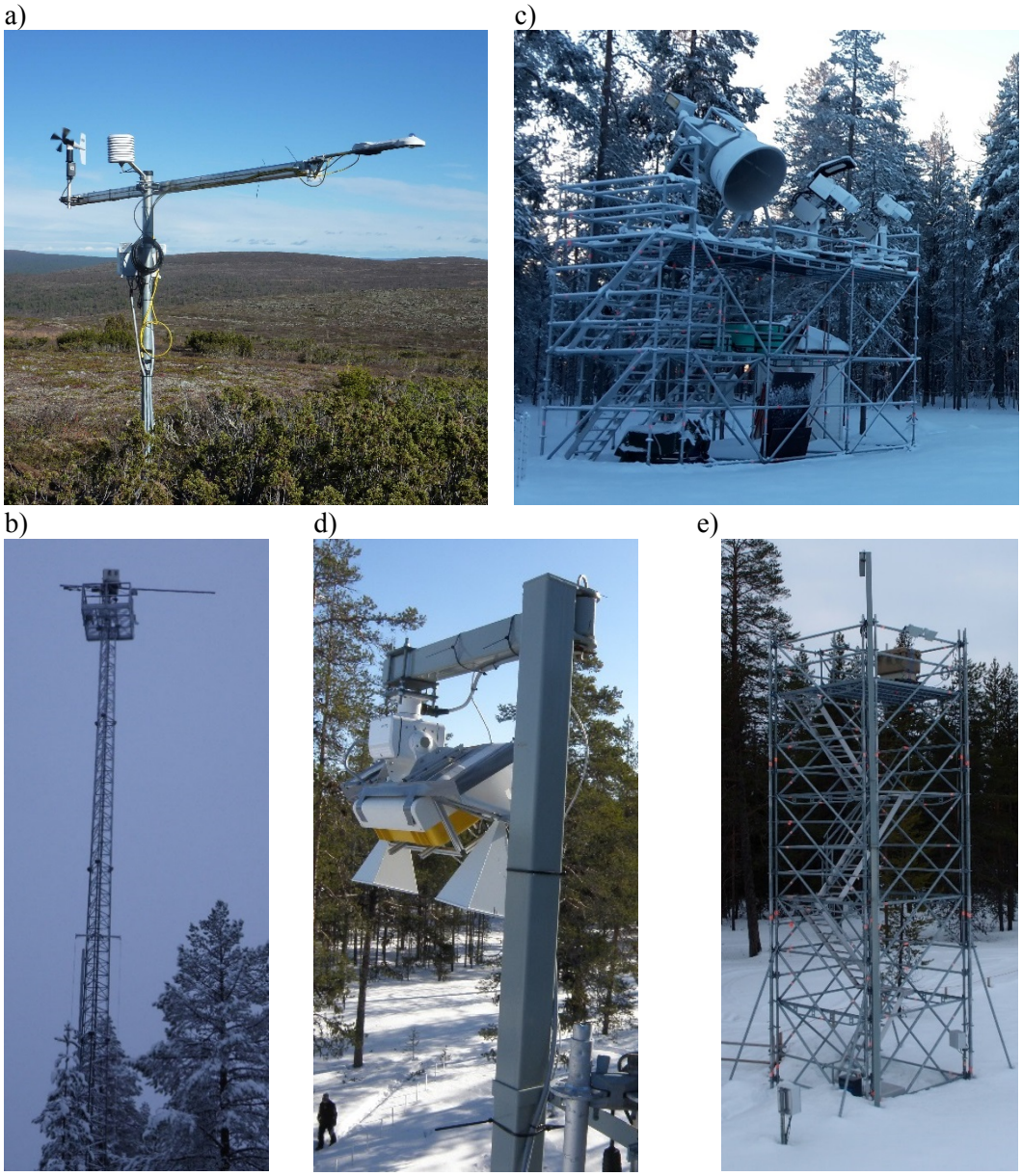

Fig. 3. a) CNR4 albedometer at Saariselkä. Thermometer and wind sensor are installed on the same bar, b) optical spectoradiometer FieldSpec Pro JR installed on 30 m mast, c) ESA ELBARA-II, SodRad1 and SodRad2 radiometers on 4 m tower, and d) ESA SnowScat scatterometer and e) SodScat scatterometer on 8 m tower.

3 *Comparison of manual and automated measurements*

3.1 *Snow depth analysis*

Automated snow depth measurements from the two SR50 sensors at the IOA are compared to manual observations (Fig. 4 and Fig. 5). The manual observations are made weekly (biweekly 2014–2015) using fixed stakes (*Leppänen et al.*, 2016). Five fixed stakes were installed in 2009 in the clearing and two stakes were added in 2010. At the same time, ten stakes were installed in the forest. The manual observations of each date are averaged for clearing and forest. Average bias for 2009–2017 is 4.1 cm for clearing and 7.2 cm for forest so that the manual observation are larger than the automated observations. The large difference of bias values is expected to originate from spatial variability and growth of forest floor vegetation (*Leppänen and Leinss*, 2017). The correlation coefficient for clearing is 0.99 (p-value <0.001) and for forest 0.97 (p-value <0.001). Probability value, called as p-value, is the probability for the statistical hypothesis, and p-value < 0.05 describes a significant correlation.

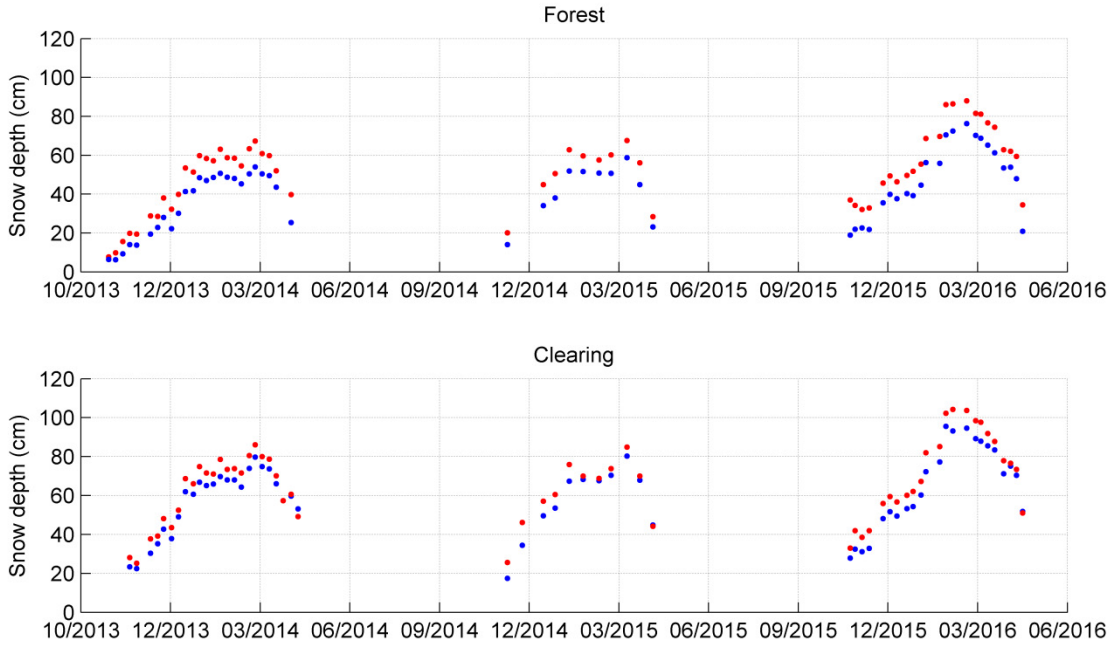

Fig. 4. Automated SR50 (blue) and manual (red) snow depth observations at IOA in forest and in clearing in 2013–2016. Automated measurements are plotted only for the same dates as the manual observations.

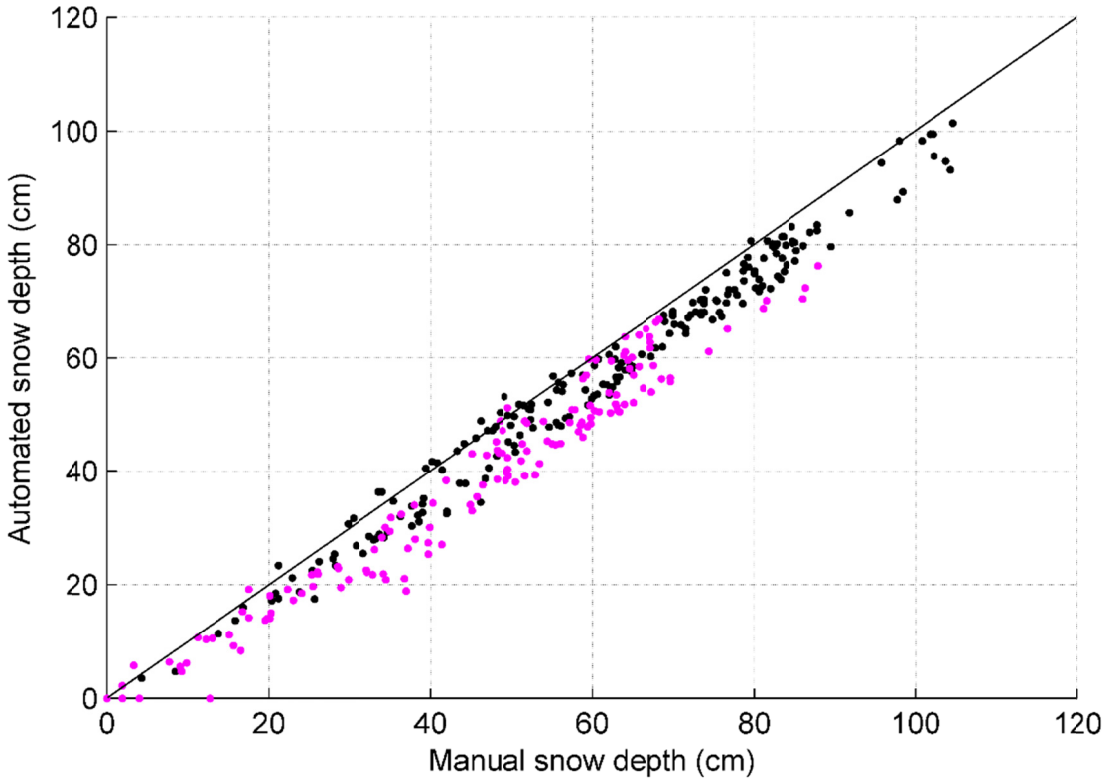

Fig. 5. Snow depth measured automatically and manually for clearing (black) and forest (magenta) in 2009–2017.

3.2 SWE analysis

Automated SWE observations of SSG1000 are compared with weekly manual SWE observations from snow pit at IOA in Fig. 6 (the GWI observations at the IOA were not available from that winter). The manual measurement is made with a Korhonen-Melander snow sampler since 2007 at the IOA (*Leppänen et al.*, 2016). If three dates are removed from the analysis from 2015–2017, when the difference between automated and manual observation was more than 20 %, correlation coefficient is 0.99 (p-value <0.001) and the average bias is 0.2 mm so that automated observation is larger than the manual. If six dates, when the difference was more than 10 % are removed, values are 0.99 for the correlation coefficient and 1.0 mm for the bias.

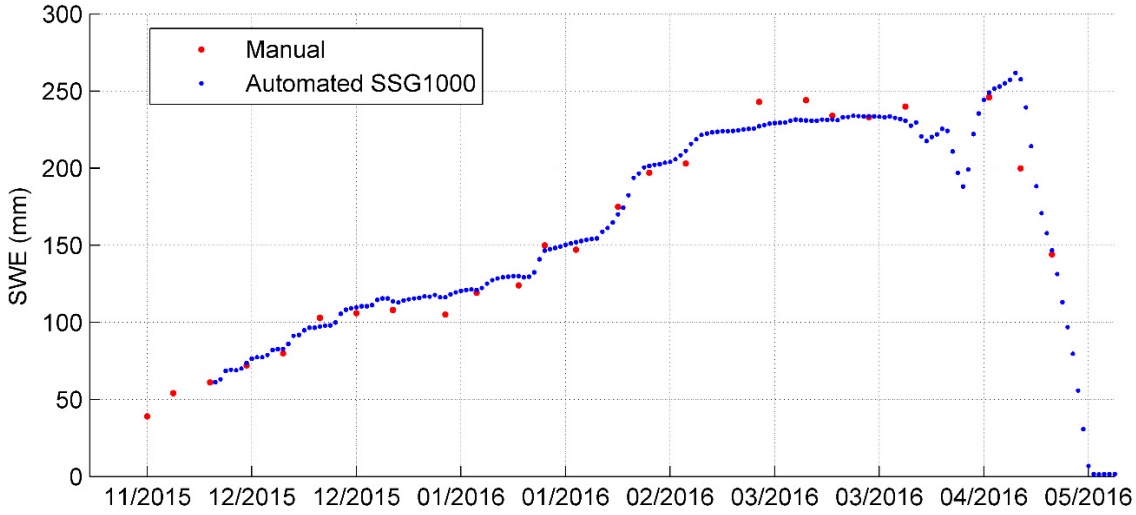

Fig. 6. Time series of SSG1000 and manually measured SWE for 2015–2016.

3.3 Snow temperature profile analysis

Snow temperature was measured both manually and automatically at the IOA in 2011–2016. Time series of the measurements is presented in Fig. 7 for measurements from 20, 30 and 40 cm heights for the dates in 2013–2015 when the snow pit measurements were made. Correlation coefficient varies between 0.89 and 0.97, and RMS error is from 0.7 °C to 2.2 °C (Table 2). The average bias is between 0.1 and 0.5 °C so that automatically measured temperature is larger than the manual observation.

Table 2. Bias, RMSE, correlation coefficient (R) and p-value between automated and manual snow temperature observations from 20, 30 and 40 cm heights.

	Height (cm)	Bias (°C)	RMSE (°C)	R	p-value
2013–14	20	0.4	1.2	0.90	<0.001
	30	0.5	1.5	0.89	<0.001
	40	0.7	2.0	0.94	<0.001
	Average	0.55	1.61	0.91	
2014–15	20	0.2	0.7	0.97	<0.001
	30	0.2	1.3	0.96	<0.001
	40	-0.2	2.2	0.95	<0.001
	Average	0.12	1.50	0.96	

Fig. 7. Snow temperature measured automatically and manually at 20, 30 and 40 cm heights from the ground. Automated measurements are plotted only for the same dates as the manual observations.

4 Discussion

The comparison of automated and manual snow depth measurements shows that there is a very good correlation between the measurements. There is less snow in the forest than on the clearing, which is expected as the trees intercept some of the falling snow. The difference is on average 19.0 cm in automated and 14.5 cm in manual measurements for the period 2013–2016. However, the forest have an average bias of 7.2 cm and the clearing have average bias of 4.1 cm (total average bias is 5.6 cm) between manual and automated observations for 2009–2017. Snow depth varies even in the small area due to forest and low vegetation, uneven ground surface and instrument installations. That explains the large bias value in the forest, since distance between automated and manual observations is larger than in the clearing. The growing vegetation also causes difference between the observations over long periods of time (*Leppänen and Leinss*, 2017). There are no vegetation at the artificial turf target of the automated sensor, but the fixed manual stakes have some low vegetation such as lichen and heather around them. The artificial turf and its wooden support frame used as a target for the automated measurement has different heat conductivity than the natural soil. Therefore thin snow layers melt fast from the target. In addition, in spring the snowmelt begins from around object protruding above snow surface, such as trees and the support pole for automated instruments. This would explain at least part of the difference in measurements. The snow stakes also accumulate snow around them and cause snow melting

in spring creating a pit around the stake. This is taken into account by removing accumulated snow and reading the snow depth from the surface level, but still they complicate measurements and may induce inaccuracy.

The bias of the SSG1000 SWE measurements is very low, only 0.2–1.0 mm for two winters in 2015–2017, if values diverging by 10–20 % (suspected bridging effect) are removed. In 2016, there is one sample during the melting period when the automated SWE measurement is ~60 mm higher than the manual. However, as visible in Fig. 6, the automated value decreases to the same level with the manual measurements in three days. This case is probably a result of uneven snowmelt and spatial variability, even though the distance between the measurements is less than 10 m. In addition, the fact is that snow melts earlier and faster from the snow pit area than from the surroundings. Snow in Sodankylä is so soft that it compacts when a snow pit is dug, and after measurements the compacted snow is not enough to fill the excavated pit. Therefore there is less snow on the area where the pits have been dug and the bare ground is revealed earlier. We expected ice bridging to explain the two points during snow maximum in March 2016, when manual measurement has shown clearly higher SWE value than the automated. However, meteorological conditions did not favor bridging, and these two points are probably just due to spatial differences in SWE. *Smith et al*. (2017) presented similar correlation coefficient values and mean relative bias values of -11-8 % between manual measurements and SSG1000 observations.

The average RMSE of snow temperature profile measurements is 0.3 ^{o}C when automated and manual observations are compared from 20, 30 and 40 cm heights for 2013–2015. Generally, the automated temperature is larger than the manual. The difference originates from sensor accuracy and accuracy of manual measurements, which depends on the thermal equalization and the horizontal perpendicular position of thermometer against the snow pit wall. This study does not include measurements from ground surface and 10 cm height, because those values have variability originating from vegetation in both the automated and the manual observations. In addition, the snow depth might have small differences between the measurement locations. As visible in April 2014 and 2015, automated temperatures are positive and indicate that the sensors located above the snow surface due to melting around the support structure. The automated measurement has the error related to the accumulation and pit formation around the sensors as described earlier. Therefore, the comparison excluded values above 40 cm to reduce effect of snow surface level at the automated station. Although, the correlation is strong for automated and manual observations with average correlation coefficient of 0.93.

Future work is concentrated on the development and validation of remote sensing instrumentation and development of interpretation algorithms. Therefore, microwave instruments (ESA ELBARA-II, SodRad1, SodRad2 and SodScat) were moved to the ICOS tower in 2018. The second up-looking ESA ELBARA-II instrument was installed on the ground next to the tower. In addition, an optical hyperspectral camera (Rikola, Senop) with a wavelength range of 300–900 nm will be installed to the same tower in 2019. The aim of the experiment is to observe the forest canopy with optical and mi-

crowave instruments to detect the effect of forest to the observations for remote sensing related purposes. Automated reference snow measurements exist in the vicinity of the ICOS tower at the micrometeorological mast site (snow depth and snow temperature profile), automated SWE instrument was installed to the ICOS tower site and weekly manual snow pit measurements will be made at the site. In addition to the presented methods, web-cameras can be used to detect snow presence and snow extent in the future (*Arslan et al*., 2017). Web-cameras are already installed to most of the sites, but not yet utilized for that purpose.

5 Summary

Continuous automated snow measurements complement the data collected in regular manual snow pit measurements and snow courses at the Arctic Space Centre of Finnish Meteorological Institute (*Leppänen et al*., 2016). The first automated measurements were snow depth and snow temperature profile at the meteorological mast site in 2000 as ancillary data for carbon flux observations. Since 2006 both manual and automated observations have been made more intensively for research purposes such as calibration, validation and development of remote sensing instrumentation and interpretation algorithms for global observations of the cryosphere. After 2006 the collection of snow instruments has been constantly expanded. Availability of the datasets are described in http://litdb.fmi.fi.

The automated measurements are compared with the manual observations to study the accuracy of the automated measurements. The results confirmed that correlation between manual and automated measurements is good with the average correlation coefficients of 0.98 for the snow depth, 0.99 for the SWE and 0.93 for the snow temperature profile. However, some bias exists for snow depth (7.9 cm, ~10%) and for temperature profile (0.3 ^{o}C, ~10%). The bias for automated SWE is only 1 mm (~2%). Spatial changes in snowpack, variability originating from use of the manual instrumentation, and errors of the automated observations are the most important factors causing differences between the manual and the automated observations. This study confirms the usability of the presented automated methods to observe snow depth, SWE and snow temperature. Previous studies have compared microwave brightness temperature and backscattering observations with simulations based on in-situ snow observations (*Maslanka et al*., 2016; *Kontu et al*., 2017; *Leinss et al*., 2015; *Sandells et al*., 2017; *Lemmetyinen et al*., 2018) highlighting the need for good-quality reference measurements for model and algorithm development for the utilization of satellite measurements. In addition, tower-based optical reflectance observations have been compared with in-situ reflectance observations for snow mapping purposes (*Salminen et al*., 2009). Continuous development of novel technology enables new applications for more accurate automated snow observations. In the future, automated measurements give the possibility to extend spatial coverage of key cryosphere variables for several purposes as hydrological modelling, numerical weather prediction and remote sensing.

Acknowledgements

We thank the personnel of FMI-ARC, who participated manual observations, and installation and maintenance of the automated snow measurements. The manuscript preparation was supported in part by the Vilho, Yrjö and Kalle Väisälä Foundation of the Finnish Academy of Science and Letters. We thank Craig Smith and an anonymous reviewer for their comments to improve this paper.

References

Arslan, A.N., C.M. Tanis, S. Metsämäki, M. Aurela, K. Böttcher, M. Linkosalmi and M. Peltoniemi, 2017. Automated Webcam Monitoring of Fractional Snow Cover in Northern Boreal Conditions. *Geosciences*, **7**, 55. 10.3390/geosciences7030055

Barnett, T.P., J.C. Adam and D.P. Lettenmaier, 2005. Potential impacts of a warming climate on water availability in snow-dominated regions. *Nature*, **438**(7066), 303–309.

Bell, V.A., A.L. Kay, H.N. Davies and R.G. Jones, 2016. An assessment of the possible impacts of climate change on snow and peak river flows across Britain. *Climatic Change*, **136**, 539–553.

Engeset, R., H. Sorteberg, and H. Udnaes, Snow pillows: Use and verification, in: Snow Engineering: Recent Advances and Developments. Proceedings of the Fourth International Conference on Snow Engineering, Trondheim, Norway, 19–21 June 2000, edited by: Hjorth-Hansen, E., HOLAND, I., Loset, S., and Norem, H., AA Balkema, Rotterdam, Netherlands, 45–51.

Hall, A. and X. Qu, 2006. Using the current seasonal cycle to constrain snow albedo feedback in future climate change. *Geophysical Research Letters*, **33**, 1–4.

Hernández-Henríquez, M.A., S.J. Déry and C. Derksen, 2015.Polar amplification and elevation-dependence in trends of Northern Hemisphere snow cover extent, 1971–2014, *Environ. Res. Lett.,* **10**, 044010, doi:10.1088/1748-9326/10/4/044010.

Ikonen, J., J. Vehviläinen, K. Rautiainen, T. Smolander, J. Lemmetyinen, S. Bircher and J. Pulliainen, 2015. The Sodankylä in-situ soil moisture observation network: an example application to Earth Observation data product evaluation. *Geoscientific Instrumentation, Methods and Data Systems Discussions*, **5**, 599–629.

Janowicz, J.R., S.L. Stuefer, K. Sand and L. Leppänen, 2017. Measuring winter precipitation and snow on the ground in northern polar regions. *Hydrology Research,* **48**(4), 884–901.

Kontu, A., J. Lemmetyinen, J. Vehviläinen, L. Leppänen and J. Pulliainen, 2017. Coupling SNOWPACK-modeled grain size parameters with the HUT snow emission model. *Remote sensing of environment*, **194**, 33–47.

Lehning, M., P. Bartelt, B. Brown, T. Russi, U. Stöckli and M. Zimmerli, 1999. SNOWPACK model calculations for avalanche warning based upon a new network of weather and snow stations. *Cold Regions Science and Technology,* **30**(1–3), 145–157.

Leinss, S., A. Wiesmann, J. Lemmetyinen and I. Hajnsek, 2015. Snow water equivalent of dry snow measured by differential interferometry. *IEEE Journal of Selected Topics in Applied Earth Observations and Remote Sensing*, **8**(8), 3773–3790.

Lemmetyinen, J., C. Derksen, H. Rott, G. Macelloni, J. King, M. Schneebeli, A. Wiesmann, L. Leppänen, A. Kontu, and J. Pulliainen, 2018. Retrieval of Effective Correlation Length and Snow Water Equivalent from Radar and Passive Microwave Measurements. *Remote Sensing*, **10**(2), 170.

Lemmetyinen, J., M. Schwank, K. Rautiainen, A. Kontu, T. Parkkinen, C. Mätzler, A. Wiesmann, U. Wegmüller, C. Derksen, P. Toose, A. Roy and J. Pulliainen, 2016a. Snow density and ground permittivity retrieved from L-band radiometry: Application to experimental data. *Remote sensing of environment*, **180**, 377–391.

Lemmetyinen, J., A. Kontu, J. Pulliainen, J. Vehviläinen, K. Rautiainen, A. Wiesmann, C. Mätzler, C. Werner, H. Rott, T. Nagler, M. Schneebeli, M. Proksch, D. Schüttemeyer, M. Kern and M.W.J. Davidson, 2016b. Nordic Snow Radar Experiment, *Geosci. Instrum. Method. Data Syst.,* **5**, 403–415. doi:10.5194/gi-5-403-2016.

Lemmetyinen, J., C. Derksen, P. Toose, M. Proksch, J. Pulliainen, A. Kontu, K. Rautiainen, J. Seppänen and M. Hallikainen, 2015. Simulating seasonally and spatially varying snow cover brightness temperature using HUT snow emission model and retrieval of a microwave effective grain size. *Remote Sensing of Environment*, **156**, 71–95.

Lemmetyinen, J., J. Pulliainen, A. Rees, A., Kontu, Y. Qiu and C. Derksen, 2010. Multiple-layer adaptation of HUT snow emission model: Comparison with experimental data. *IEEE Transactions on Geoscience and Remote Sensing*, **48**(7), 2781–2794.

Leppänen, L., A. Kontu, H.-R. Hannula, H. Sjöblom and J. Pulliainen, 2016. Sodankylä manual snow survey program. *Geosci. Instrum. Methods Data Syst*., **5**, 163–179.

Leppänen, L., A. Kontu, H-R. Hannula, H. Sjöblom and J. Pulliainen, 2016. Sodankylä manual snow survey program. *Geoscientific Instrumentation, Methods and Data Systems,* **5**(1), 163–179.

Maslanka, W., L. Leppänen, A. Kontu, M. Sandells, J. Lemmetyinen, M. Schneebeli, M. Proksch, M. Matzl, H-R. Hannula and R. Gurney, 2016. Arctic Snow Microstructure Experiment for the development of snow emission modelling. *Geoscientific Instrumentation, Methods and Data Systems*, **5**(1), 85–94.

Niemi, K., S. Metsämäki, J. Pulliainen, H. Suokanerva, K. Böttcher, M. Leppäranta and P. Pellikka, 2012. The behaviour of mast-borne spectra in a snow-covered boreal forest. *Remote sensing of environment*, **124**, 551–563.

Pirinen, P., H. Simola, J. Aalto, J.-P. Kaukoranta, P. Karlsson and R. Ruuhela, 2012. Climatological statistics of Finland 1981–2010, *Finnish Meteorological Institute reports*.

Pulliainen, J., M. Salminen, K. Heinilä, J. Cohen and H.-R. Hannula, 2014. Semi-empirical modeling of the scene reflectance of snow-covered boreal forest: Validation with airborne spectrometer and LIDAR observations. *Remote sensing of environment*, **155**, 303–311.

Rautiainen, K., T. Parkkinen, J. Lemmetyinen, M. Schwank, A. Wiesmann, J. Ikonen, C. Derksen, S. Davydov, A. Davydova, J. Boike and M. Langer, 2016. SMOS prototype algorithm for detecting autumn soil freezing. *Remote sensing of environment*, **180**, 346–360.

Rautiainen, K., J. Lemmetyinen, M. Schwank, A. Kontu, C. B. Ménard, C. Mätzler, M. Drusch, A. Wiesmann, J. Ikonen and J. Pulliainen, 2014. Detection of soil freezing from L-band passive microwave observations. *Remote Sensing of Environment*, **147**, 206–218.

Rautiainen, K., J. Lemmetyinen, J. Pulliainen, J. Vehvilainen, M. Drusch, A. Kontu J. Kainulainen and J. Seppänen, 2012. L-band radiometer observations of soil processes in boreal and subarctic environments. *IEEE Transactions on Geoscience and Remote Sensing*, **50**(5), 1483–1497.

Rittger, K., T.H. Painter and J. Dozier, 2013. Assessment of methods for mapping snow cover from MODIS. *Advances in Water Resources*, **51**, 367–380.

de Rosnay, P., G. Balsamo, C. Albergel, J. Muñoz-Sabater and L. Isaksen, 2012. Initialisation of land surface variables for numerical weather prediction. *Surveys in Geophysics*, **35**(3), 607–621.

Salminen, M., J. Pulliainen, S. Metsämäki, A. Kontu and H. Suokanerva, 2009. The behaviour of snow and snow-free surface reflectance in boreal forests: Implications to the performance of snow covered area monitoring. *Remote Sensing of Environment*, **113**(5), 907–918.

Sandells, M., R. Essery, N. Rutter, L. Wake, L. Leppänen, and J. Lemmetyinen, 2017. Microstructure representation of snow in coupled snowpack and microwave emission models. *The Cryosphere*, **11**(1), 229–246.

Smith, C. D., A. Kontu, R. Laffin and J.W. Pomeroy, 2017. An assessment of two automated snow water equivalent instruments during the WMO Solid Precipitation Intercomparison Experiment. *The Cryosphere,* **11**(1), 101.

Sukuvaara, T., J. Pulliainen, E. Kyrö, H. Suokanerva, P. Heikkinen and J. Suomalainen, 2007. Reflectance spectroradiometer measurement system in 30 meter mast for validating satellite images. *In Geoscience and Remote Sensing Symposium, 2007. IGARSS 2007. IEEE International* (pp. 2885–2889).

Schwank, M., A. Wiesmann, C. Werner, C. Mätzler, D. Weber, A. Murk, I. Völksch and U. Wegmüller, 2010. ELBARA II, an L-band radiometer system for soil moisture research. *Sensors*, **10**(1), 584–612.

Takala, M., J. Ikonen, K. Luojus, J. Lemmetyinen, S. Metsämäki, J. Cohen, A.N. Arslan and J. Pulliainen, 2017. New snow water equivalent processing system with improved resolution over Europe and its applications in hydrology, *IEEE Journal of Selected Topics in Applied Earth Observations and Remote Sensing*, **10**(2), 428–436.

Tietäväinen, H., H. Tuomenvirta and A. Venäläinen, 2010. Annual and seasonal mean temperatures in Finland during the last 160 years based on gridded temperature data, *Int. J. Climatol*., **30**, 2247–2256.

Vormoor, K., D. Lawrence, M. Heistermann and A. Bronstert, 2015. Climate change impacts on the seasonality and generation processes of floods – projections and uncertainties for catchments with mixed snowmelt/rainfall regimes. *Hydrol. Earth Syst. Sci.*, **19**, 913–931.

Wiesmann, A. and C. Mätzler, 1999. Microwave emission model of layered snowpacks. *Remote Sensing of Environment*, **70**(3), 307–316.

Wiesmann, A., C. Werner, T. Srozzi, C. Matzler, T. Nagler, H. Rott, M. Schneebeli and U. Wgmuller, 2010. SnowScat, X-to Ku-band scatterometer development. ESA Living Planet Symposium (Vol. 686), ISBN 978-92-9221-250-6.

Xie, S. P., C. Deser, G. A. Vecchi, M. Collins, T. L. Delworth, A. Hall, E. Hawkins, N. C. Johnson, C. Cassou, A. Giannini and M. Watanabe, 2015. Towards predictive understanding of regional climate change. *Nature Climate Change*, **5**(10), 921.